Andrzej Zieliński
Gdansk University of Technology, Gdansk, Poland
Małgorzata Warmuzek, Andrzej Gazda
Foundry Research Institute, Cracow, Poland
Elżbieta Jezierska
Warsaw University of Technology, Warsaw, Poland
Jacek Chrzanowski
Ship Design and Research Centre, Gdansk, Poland

INFLUENCE OF RETROGRESSION AND REAGING (RRA) HEAT TREATMENT ON MICROSTRUCTURE, MECHANICAL AND CHEMICAL BEHAVIOUR OF AN Al–Zn–Mg ALLOY

ABSTRACT

The Al-Zn-Mg alloy of the T6 temper alone or followed by the retrogression and Reaging heat treatment was investigated. The mechanical properties were determined with the slow strain rate test in air or substitute sea water environments, and fracture energy, elongation and RA calculated. The fracture faces after the tensile tests were examined with the SEM. The microstructure and dislocation network were examined with the TEM. The heat treatment affected the investigated features: alloy subject only to the T6 temper demonstrated the best mechanical properties and the highest susceptibility to stress corrosion cracking. The increase in retrogression temperature and decrease in retrogression time positively influenced the resistance to SCC. The observed effects were explained by change in microstructure which caused changes in hydrogen diffusion and trapping, and then initiation and propagation of cracks..

INTRODUCTION

The 7xxx precipitation-hardened Al-Zn-Mg alloys have been used o build some elements of aluminium high speed boats, navy ships, yachts, etc. However, the long term application of the most popular AA7010 alloy has disclosed its disadvantages: susceptibility to exfoliation (layer) corrosion, corrosion fatigue, stress corrosion cracking, especially for welded joints in contact with sea water [1-7]. Therefore, in spite of better mechanical properties of raw materials they are replaced by traditional 5xxx Al-Mg. Additionally, new similar alloys or new heat treatments are still looking for.

For the 7010 alloy the T6 temper composed of one or two-stage artificial aging following solution heat treatment is generally applied. For the non-weldable precipitation-hardened Al-Zn-Mg-Cu 7075 alloy, used mainly in aerospace industry, the new heat treatment, Retrogression and Reaging, has been proposed after the T6 temper [8-15]. The idea of this treatment is based on assumption of the important role played by dislocation network in area of grain boundaries.

The retrogression is the heating stage at such temperature at which phase precipitates may dissolve and dislocation density may decrease as compared to that obtained after heat solution treatment. Such treatment results in structure resistant to stress corrosion cracking and corrosion fatigue but possessing low mechanical properties. The reaging is made at the same temperature as primary aging, in order to obtain structure with the appearing η phase precipitates and higher mechanical strength properties. Such multi-stage heat treatment allows for dissolution of unstable precipitates and precise modification of the grain boundary η phase precipitates: change in their shape, size and electrochemical properties. The high dislocation density has been suggested to be responsible for susceptibility to environmental degradation to greater extent than the kind, size and distribution of phase precipitates; following low dislocation density due to the reaging heat treatment, the sufficient resistance to environmental degradation could be achieved.

The new RRA heat treatment has been successfully explored for copper containing 7xxx aluminium alloys but never investigated for copper-free 7x weldable for which nucleation of phase precipitates is more difficult than for Al-Zn-Mg-Cu alloys. The aim of present work has been to determine whether such heat treatment may influence mechanical and chemical properties of the typical AlZn5Mg1 alloy, and how the possible changes in properties relate on microstructure and dislocation structure.

EXPERIMENTAL PROCEDURE

Chemical composition and heat treatment

The AlZn5Mg1 alloy was investigated, of following chemical composition: 4.70%Zr, 1.30%Mg, 0.24%Mn, 0.14%Cr, 0.08%Ti, 0.07%Zr, 0.30%Si, 0.35%Fe, 0.10%Cu. The alloy was delivered in the standard T6 temper heat treatment.

Upon the base of literature survey and previous DTA measurements on Al-Zn-Mg-Cu alloys the following heat treatment procedures were established: homogenization at 728 K for 5 h, solution heat treatment at 743 K for 1 h, and two different procedures of artificial aging separated by retrogression, as shown in Table 1.

Table 1. *Parameters of aging and retrogression heat treatment*

Heat treatment No.	Aging	Retrogression	Re-aging
1	403 K 16 h	453 K 1 h	403 K 16 h
2	403 K 16 h	473 K 1800 s	403 K 16 h
3	403 K 16 h	493 K 900 s	403 K 16 h
4	403 K 16 h	513 K 600 s	403 K 16 h
5	403 K 16 h	513 K 600 s	403 K 48 h
6	363 K 24 h	513 K 600 s	363 K 24 h
7	363 K 24 h	513 K 600 s	363 K 48 h
8	403 K 16 h	none	none
9	363 K 24 h	none	none

The homogenization and solution heat treatment were made in the Multitherm N 21/M heat oven (Nabertherm) with a use of preliminary vacuum system and heating in pure argon. Afterwards, the specimens were cooled in distilled water of ambient temperature and aged at similar temperature for 0.5 h. The aging, re-aging and retrogression were made in the laboratory dryer. After retrogression the specimens were cooled in water and immediately subjected to re-aging.

Mechanical slow strain tests

The tensile slow strain rate tests were made at relative strain rate 10^{-6} s^{-1} in either substitute sea water (type A according to the Polish standard) or in laboratory air. The fracture energy and time to failure during slow strain rate test, and reduction in area after the test were determined. The four independent tests were made for every heat treatment. The wiew of the research equipment is shown in Photo 1.

Microscopic examinations

The fractographic examinations were made with the STEREOSCAN 420 scanning electron microscope. The observations of microstructures and dislocation structure were made with the Hitachi transmission electron microscope on the foils prepared from tested specimens.

RESEARCH RESULTS

Effect of heat treatment on mechanical behavior

The results of tensile tests are shown in Table 2 and in Figs. 1-3. The best mechanical properties demonstrated the alloy no subject to RRA treatment, better for lower temperature and longer time of aging (No. 9).

The RRA heat treatment which has followed the higher temperature primary aging (No. 8) resulted in worse mechanical properties. The different RRA conditions, temperature and time of heat treatment, had small effects on mechanical behavior.

Table 2. *Results of slow strain rate tests*

Heat treatment No.	Fracture energy E_f [MJ/m^3]		Time to failure t_f [h]		Reduction-in-area R_a [%]	
	air	sea water	air	sea water	air	sea water
1	42.99	39.35	35.10	30.45	26.29	20.99
2	33.67	35.60	29.64	28.24	20.82	20.50
3	37.36	36.86	31.79	30.48	24.97	21.63
4	39.54	38.12	33.04	30.53	21.78	20.32
5	37.83	37.15	30.81	30.54	21.84	20.83
6	60.40	59.76	48.08	47.04	31.57	29.23
7	57.63	52.22	44.02	41.69	28.35	26.04
8	50.57	45.83	43.07	37.59	28.17	24.17
9	87.12	65.94	57.93	45.65	30.81	27.32

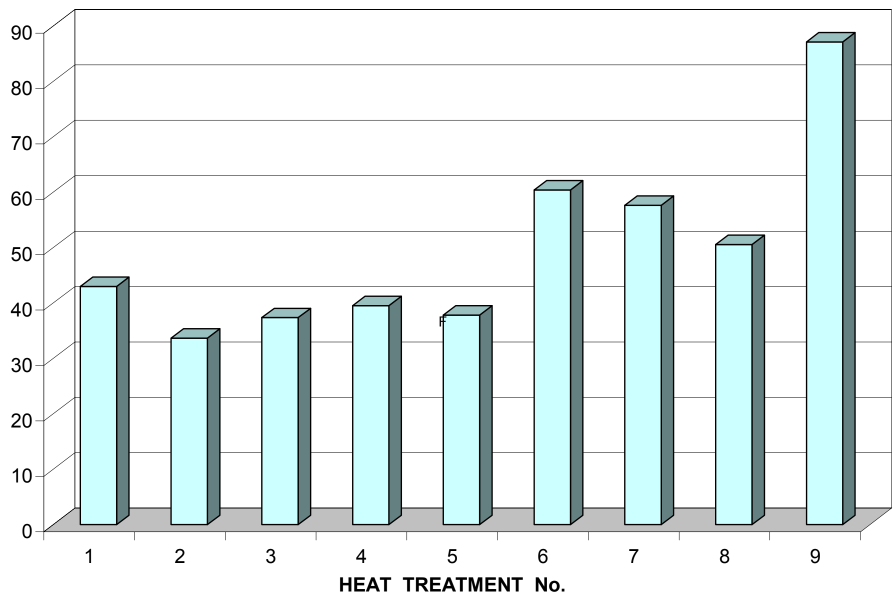

Fig. 1. Effect of heat treatment on fracture energy in slow strain rate test in air

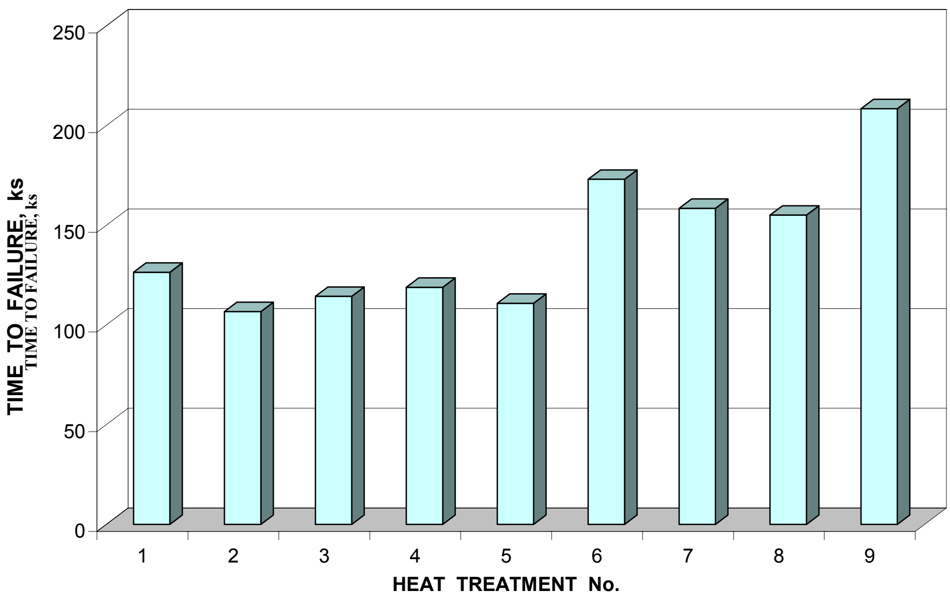

Fig. 2. Effect of heat treatment on time to failure in slow strain rate test in air

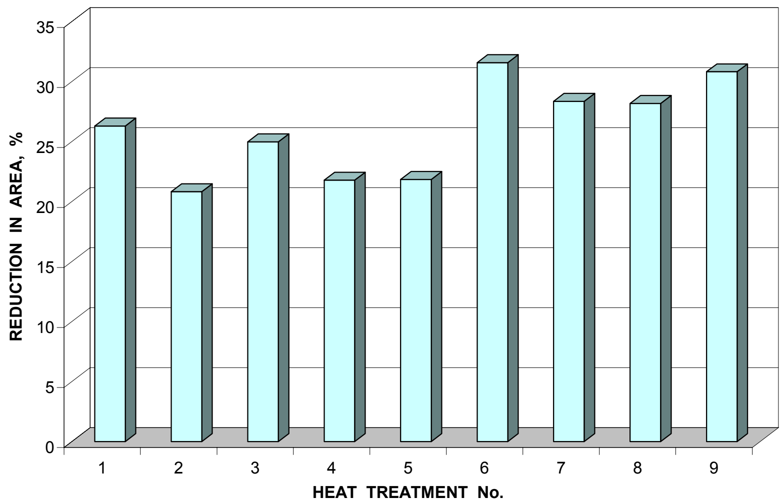

Fig. 3. Effect of heat treatment on reduction in area in slow strain rate test in air

Effect of heat treatment on susceptibility to stress corrosion cracking (SCC)

Upon the base of slow strain rate tests, the index of susceptibility of the alloy to stress corrosion cracking I_{SCC} was calculated as:

$$I_{SCC} = (1 - P_c / P_a)$$

where P_a and P_c mean the value of each of measured properties (fracture energy, reduction-in-area, time to failure) in air and corrosion solution, respectively.

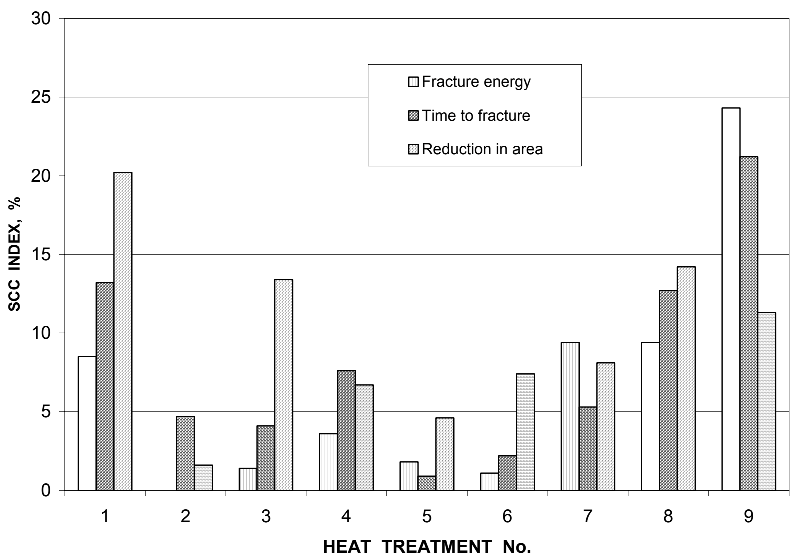

Fig. 4. Effect of heat treatment on SCC index in slow strain rate test in sea water

The estimated values of SCC index are shown in Fig. 4. The highest susceptibility to SCC was demonstrated by alloy no subject to any RRA treatment (Nos. 9 and No. 8). The application of RRA heat treatment (Nos. 1 to 7) resulted in distinct decrease in SCC susceptibility; the higher temperature and shorter time of retrogression, the lowest susceptibility index. The increase in reaging time had negative effect on resistance to SCC for alloy aged at 363 K and positive effect for alloy aged at higher 403 K temperature (cf. Nos. 7 and 6, and Nos. 4 and 5).

Fractographic examinations

Photos 2-44 illustrate the fracture surface morphology of the alloy subject to different heat treatment and tensed in air or in sea water.

For the alloy following heat treatment No. 2 tensed in air the fracture surfaces were much more developed than in sea water (or aged at 363 K without any RRA treatment) (Photo 2). The shear areas (Photo 3) were placed mainly at the surface of the specimen, and only locally at the centre (Photo 4). The terrace arrangement of the shear regions was dominant. The observed steps can be considered as the initial stage of the secondary cracks formation. For the alloy subject to heat treatment No. 2 tested in sea water, the areas of pure shearing were surrounded by equiaxial holes, characteristic of local tension (Photos 5-8). No preferred shearing direction was observed in the whole cross section.

After heat treatment No. 3 the very developed fracture surface of specimens tensed in air (Photo 9) indicates an important material deformation. In ductile fracture zones the deep equiaxial dimples, partly in shear bands, appeared around the η phase particles of different dispersion. Close to the specimen rim the shear process was more advanced, and the visible dimples – distinctly more shallow. In sea water (Photos 10-12) the band arrangement of dimples (11) and numerous discontinuities associated with presence of precipitates (12) were observed. The striations appeared between shear areas of deformed matrix. The fracture surface was less developed near the surface: the dimples were more shallow and their bands separated by bands of sheared matrix (12).

For the alloy subject to heat treatment No. 5 tensed in air (Photos 13-16) the ductile fracture was observed in central zone; morphology was characteristic for the ductile one. The bands of equiaxial and oval dimples appeared as a result of progressed deformation of the α-Al solid solution (Photos 13, 14). The tear ridges were observed between the dimple bands, situated in the microareas of local matrix deformation, together with visible precipitates of intermetallic phases. The initial decohesion took place at the interfaces between η phase particles and α-Al solid solution. At the specimen rim the fracture morphology revealed other features (Photo 13): the broad shear areas are present (Photos 15, 16) surrounded by places in which the dimple zones formed as a result of the shearing of initial voids. The secondary cracks were formed (Photo 14). For sea water tests the large areas of sheared solid solution and bands formed by gropus of sheared dimples were observed (Photo 17). The microareas of local decohesion appeared at the interphase boundaries η/α. Some oxide inclusions were observed (Photo 18).

For the alloy tensed in air after heat treatment No. 6 (Photos 19-23) the fracture surface was less developed than in air. The dimples in the region of the ductile fracture were more shallow (Photos 20, 22), and major part of the fracture surface was occupied by the shearing areas of solid solution (Photos 21, 23). In sea water tests (Photos 24-27) the deformation of matrix was followed by fracture of solid solution as confirmed by dimples and different stages of microvoids` coalescence (Photoso 24, 25). The initiation of microdeformations associated with ductile fracture of matrix occurred around the $MgZn_2$ particles (Photos 26, 27). The shearing had a local character but the preferred propagation direction was observed.

For heat treatment No. 7 the fracture surface was not very developed in air tests (Photos 28-31). The dimples characteristic of ductile fracture appeared mainly at the specimen centre. The very disperse η phase precipitates initiated the microvoids` formation in the areas of ductile fracture while the massive particles made the barriers for these cracks propagation, by changing their path and increasing the total failure energy (Photo 29). The directed bands of the microvoids' coalescence (Photo 31) presumably constituted the initial stage of appearance of observed secondary cracks (Photo 30). In sea water tests (Photoso 32-35) the less developed fracture surface was observed (Photo 32). The dimples characteristic of ductile fracture appeared, mainly close to the specimen axis (Photo 34, 36). The presence of equiaxial dimples suggests the local straining of material at plain stress. Near the specimen surface the areas of sheared solid solution (Photo 35) were present with elongated dimples, open into the crack front propagation direction. Parallel to the crack advancement the bands of secondary line microcracks appeared (Photo 32), frequently of zig-zag character (Photos 34, 35).

For heat treatment No. 8 the fracture surface of alloy tensed in air was less developed than in sea water, with band arrangement of the microdiscontinuities (Photo 36). After sea water test (Photo 37) the morphology was similar to that observed after heat treatment No. 2 and 3: similar fracture surface development, the distinct arrangement of band dimples.

For heat treatment No. 9 the areas of ductile fracture were present, more for specimen tensed in air (Photos 38-41) than in sea water (Photos 42-44). The shear mechanism was dominant. which advanced in preferred direction in the whole cross section (Photo 38). Besides the short secondary cracks (Photos 40,41), the rectilinear cracks across the whole specimen section were present (Photo 38). In sea water test the final shearing of alloy occurred at a few different planes (Photos 42, 43). The presence of equiaxial dimples confirms the local tension at plain stress (Photo 44). As for heat treatment No. 7, the bands of secondary cracks of local character were parallel to the shear direction (Photo 44).

TEM examinations of microstructure and dislocation structure

Some results of TEM examinations are illustrated in Photos 45-53.

For heat treatment No. 1 the double boundaries with precipitates, precipitate free zones and secondary precipitates at the dislocations were observed. The matrix around the greater precipitates was impoverished, elongated precipitates were present.

For heat treatment No. 2 the secondary precipitates at the interphase boundaries and a great number of small precipitates at the dislocations and grain boundaries was observed.

For heat treatment No. 3 the impoverished matrix at the grain boundary phase precipitates appeared, a lot of small precipitates at the dislocations inside the grains and at the grain boundaries were present.

For hest treatment No. 4 at some grain boundaries the narrow precipitate free zone appeared. The very small precipitates were present at the dislocations inside the grains.

For heat treatment No. 5 the rows of precipitates along the grain boundaries were present, the very small elongated subgrains appeared.

For heat treatment No. 6 a number of grain boundary small precipitates, close to each other, were present.

For heat treatment No. 7 the primary precipitates were present at the grain boundaries and inside the grains. The dislocation density was substantial.

For heat treatment No. 8 the precipitate free zones were present. The precipitates nucleated at the dislocations.

For heat treatment No. 9 the nucleation of precipitates started at the dislocations and dislocation networks.

DISCUSSION

The obtained results show that the application of additional RRA treatment results in some changes in mechanical behaviour in inert and corrosive environments. However, it must be stated that at any case the increase in resistance to SCC is followed by fall in mechanical properties. Thus, to the contrary to Al-Zn-Mg-Cu alloy, it has become impossible to increase corrosion behavior of an Al-Zn-Mg alloy at similar mechanical properties.

Although the observed difference in behaviour of the alloy subject to various heat treatment is no remarkable, it may be explained by difference in microstructure that affects both mechanical properties and crack development in inert and corrosive solution.

The most interesting observations relate on fracture behaviour. For the alloy aged at lower 363 K and no subject to RRA treatment, the shearing of the material took place at a few surfaces at a time, at different slope towards the specimen axis, and it follows the local initiation and coalescence of microvoids at the η phase precipitates. The bands of oval shear dimples are present on the fracture surface, developed more than that after the RRA treatment. The short secondary cracks parallel to the bands of dimples appear.

The application of the RRA does not dramatically affect the fracture which is caused by complex decohesion mechanism with contribution of the matrix shearing. The fracture surface becomes less developed and inclined (as average) to the specimen axis at an angle close to 45°. The shear dimples form as a result of the local decohesion at the interfaces, and are grouped in the bands parallel to the average shear direction. As in the case of the tempered T6 alloy the long, rectilinear, secondary cracks, parallel to these dimple bands, are observed.

The microscopic examinations of the alloy aged at 363 K permit to explain the observed small differences in mechanical and chemical properties rather by different morphology of precipitates than by different dislocation structure: the most resistant microstructure possesses a great number of the very small particles. The relative resistance to SCC may be then related to the hydrogen trapping by numerous interphase boundaries, and, on the other hand, with good cohesion of precipitates to the matrix and appearance of discontinuous lines of grain boundary precipitates.

The mechanical properties of the alloy aged at 403 K are much worse than those of aged at lower temperature, and susceptibility better. The microstructures of this group is not much affected by the RRA parameters, and phase precipitates, both in matrix and along the grain boundaries are observed together with precipitate – free zone. The fracture surface of the alloys subject to the RRA heat treatment demonstrates the macroscopic ductile effect (large RA). The fracture surface is relatively well developed, and numerous shear zones are inclined at various angles to the specimen axis; at the specimen centre the inclination angle is close to 90°C. The ductile fracture caused by shearing of microvoids and development of dimples is prevalent. The shear dimples are shallow, often elongated and open.

In all tested specimens the transcrystalline ductile fracture mode was observed, with typical sheared dimples, oval or open, which resulted from the local microdeformations of the matrix around the disperse η phase precipitates, initiated by decohesion at interfaces. The shearing of matrix, locally deformed, is then important fracture mechanism.

The observed differences in susceptibility to SCC may be explained by different microstructure, taking into account the hydrogen-enhanced SCC models in the Al alloys. If the hydrogen contribution to the SCC of aluminum alloys were substantial, as usually claimed, two hydrogen transport mechanisms would be possible: lattice diffusion and dislocation transport. The hydrogen atoms moving by lattice diffusion occupy the dislocation tangles, voids and incoherent precipitates. The hydrogen atoms transported by dislocations may be also stopped at coherent precipitates. At relatively low aging temperature, 363 K, the substantial amount of coherent and semicoherent precipitates may appear, which may then constitute the additional – as compared to the microstructure obtained after 403 K aging – preferred places of hydrogen segregation and nucleation of microvoids. At such places the cracks are initiated as here observed. The appearance of such defects in alloy aged at lower temperature may by confirmed by more advanced strengthening as compared to the alloy aged at 403 K, for which the formation of neck was observed. These results indicate that the hydrogen mechanism may be then responsible for SCC of tested Al alloy.

Unfortunately, the obtained TEM results cannot confirm or reject the supposition on important role played by dislocations in grain boundary area. No substantial difference in dislocation density and behaviour was observed; however, the number of dislocations was very different in various places and therefore the dislocation density impossible to estimate and compare.

CONCLUSIONS

The Retrogression and Reaging heat treatment has a certain effect on microstructure, fracture behaviour, mechanical properties and susceptibility to stress corrosion cracking.

The observed difference well correspond to the development of grain boundary phase precipitates which affect the development of fracture surface, fracture path, initiation, propagation, number and placement of primary and secondary cracks, fracture mode. The change in dislocation network following heat treatment and the effect of grain boundary dislocations seems weak.

The initiation and development of fracture may be explained by hydrogen-enhanced stress corrosion cracking models.

REFERENCES

1. De Ardo A.J., Townsend R.D.: The effect of microstructure on the stress corrosion susceptibility of an Al-Zn-Mg alloy. Manag. Inf. Serv., Detroit 1970.
2. Christodolou L, Flower H.M.: Hydrogen embrittlement and trapping in Al-6% - Zn-3% - Mg. Acta Metall. 28, 1981, 481.
3. Holroyd N.J.H.: Environment-induced cracking of high-strength aluminum alloys. Proc. Conf. Environment-Induced Cracking, NACE, Kohler, USA, 1988, 311.
4. Holroyd N.J.H., Vasudevan A.K., Christodolou L.: Stress corrosion of high-strength aluminum alloys. Treat. Mater. Sci. Technol. 31, 1989, 463.
5. Lynch S.P.: Environmentally induced cleavage-like cracking in aluminium alloys. Proc. Conf. Corrosion - Deformation Interaction, Fontainebleau, 1992, 401.
6. Oñoro J., Ranninger C.: Exfoliation corrosion behaviour of welded high strength aluminium alloys. Brit. Corr. J. 28, No. 2, 1993, 137.
7. Braun R.: Environmentally assisted cracking of aluminium alloys. Proc. ICAA-6, vol. 1, 1998, 153.
8. Thompson J.J., Tankins E.S., Agarwalla V.S.: Stress corrosion cracking resistant heat treatment for 7000 series aluminum alloys - RRA. Proc. Conf. Environmental Degradation Engineering Materials, Houston, vol. III, 1987, 329.
9. Talianker M., Cina B.: Retrogression and reaging and the role of dislocations in the stress corrosion of 7000-type aluminum alloys. Metall. Trans. 20A, 1989, 2087.

10. Cina B.: Reducing the susceptibility of alloys, particularly aluminium alloys, to stress corrosion cracking. U.S. Patent No. 3, 856, 584, Dec 24, 1974.
11. Lacom W.: Calorimetric investigations in a dispersion strenghened 7075 alloy. Therm. Acta 271, 1996, 93-100.
12. Chinh N.Q., Kovacs Zs. et al.: Precipitation hardening in high strength AlZnMg(Cu,Zr) alloys. Mater. Sci. Eng., 1996, 1293-1298.
13. Hall M.B., Martin J.W.: The effect of retrogression temperature on the properties of an RRA (Retrogressed and Re-aged) 7150 aluminium alloys. Zeit. Metallk. 85(2), 1994, 134-139.
14. Hepples W., Jarret M.R., Crompton J.S., Holroyd N.J.H.: The influence of microstructure on the stress corrosion cracking and exfoliation of commercial Al-Zn-Mg-Cu alloys. EICM Proc., 1989, 383-387.
15. Islam M.U., W. Wallace: Retrogression and reaging response of 7475 aluminium alloy. Met. Techn. 10, 1983, 386-392.